PACS: 62.72.Bb

R.Z. Valiev

THE NEW TRENDS IN SPD PROCESSING TO FABRICATE BULK NANOSTRUCTURED MATERIALS

Institute of Physics of Advanced Materials, Ufa State Aviation Technical University
K. Marx Str., 12, Ufa, 450000, Russia
E-mail: rzvaliev@mail.rb.ru

During the last decade severe plastic deformation (SPD) has become a widely known method of materials processing used for fabrication of ultrafine-grained materials with attractive properties. Nowadays SPD processing is rapidly developing and is on the verge of a transition from lab-scale research to commercial production. This paper focuses on several new trends in the development of SPD techniques for effective grain refinement, including those for commercial alloys, and presents new SPD processing routes to produce bulk nanocrystalline materials.

1. Introduction

Recent years have seen growing interest in developing SPD processing to fabricate bulk nanostructured metals and alloys with unique properties [1–4]. This approach as an alternative to nanopowder compacting is based on microstructure refinement in bulk billets using SPD: that is, heavy straining under high imposed pressure [1]. SPD-produced nanomaterials are fully dense and their large geometric dimensions make it possible to perform thorough mechanical tests, and this is attractive for efficient practical applications. Fabrication of bulk nanostructured materials by severe plastic deformation is becoming one of the most actively developing areas in the field of nanomaterials [5,6]. SPD materials are viewed as advanced structural and functional materials of the next generation of metals and alloys [7].

Today, SPD techniques are emerging from the domain of laboratory-scale research into commercial production of various ultrafine-grained materials. This change is manifested in several ways. First, it is characterized by the fact that not only pure metals are investigated, but also commercial alloys for special applications; second, by the requirements of economically feasible production of ultrafine-grained metals and alloys. This paper considers these new trends in SPD processing and highlights some recent results on the development of the pilot

commercial production of Ti materials for medical use. We also report here new results on finding novel SPD processing routes used to produce bulk ultrafine-grained materials with a small grain size refined down to a typical nanorange of 40–50 nm and less.

2. Enhanced properties in SPD-produced nanomaterials

It is well known that grain refinement promotes mechanical strength, and thus one can expect ultrafine-grained materials to possess very high strength. Moreover, introduction of a high density of dislocations in SPD-processed nanometals may result in even greater hardening. However, all this normally decreases ductility. Strength and ductility are the key mechanical properties of any material, but they are typically opposing characteristics. Materials may be strong or ductile, but rarely both at once. Recent studies have shown that material nanostructuring may lead to a unique combination of exceptionally high strength and ductility (Fig. 1), but this task calls for original approaches [8–11].

One such new approach to the problem was suggested recently by Wang et al. [10]. They created a nanostructured copper by rolling the metal at low temperature – the temperature of liquid nitrogen – and then heating it to around 450 K. The result was a 'bimodal' structure of micrometre-sized grains (at a volume fraction of around 25%) embedded in a matrix of nanocrystalline grains. The material showed extraordinarily high ductility, but also retained its high strength. The reason for this behavior is that, while the nanocrystalline grains provide strength, the embedded larger grains stabilize the tensile deformation of the material. Other evidence for the importance of grain size distribution comes from work on zinc [12], copper [13], and aluminium alloy [14]. What is more, the investigation of copper [13] has shown that bimodal structures can increase ductility not only during tensile tests, but also during cyclic deformation. This observation is important for improving fatigue properties.

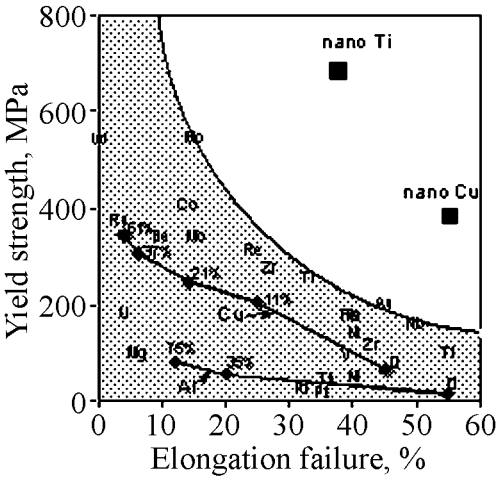

Fig. 1. Strength and ductility of the nanostructured metals compared with coarse-grained metals. Conventional cold rolling of copper and aluminium increases their yield strength but decreases their ductility. The two lines represent this tendency for Cu and Al and the % markings indicate a percentage on rolling. In contrast, the extraordinarily high strength and ductility of nanostructured Cu and Ti clearly set them apart from coarse-grained metals [8]

Another approach suggested recently [15] is based on formation of second-phase particles in the nanostructured metallic matrix, which modify shear-band propagation during straining, thereby increasing the ductility. A sys-

tematic study of both hard and soft second-phase particles with varying sizes and distributions is required here, to allow mechanical properties to be optimized.

A third approach to the problem of strength and ductility is probably the most universal of the three, because it can be applied both for metals and for alloys. The approach introduced in [1,8] is based on formation of ultrafine-grained structures with high-angle and non-equilibrium grain boundaries capable of grain-boundary sliding (GBS). It is well known that sliding, which increases ducility, normally cannot develop at low-angle boundaries. The importance of high-angle grain boundaries was verified in work [8] on the mechanical behaviour of metals subjected to different degrees of severe plastic deformation resulting in formation of various types of grain boundaries. As was noted above, sliding can be easier when non-equilibrium boundaries are present. Another example of this is the extraordinary influence of annealing temperature on mechanical behavior found recently in nanostructured titanium produced by high-pressure torsion (HPT) [16]. Here, a short annealing at 300°C results in a noticeable increase in strength combined with greater ductility than in the HPT-produced state or after annealing at higher temperature. The growth of strength and ductility was associated with higher strain-rate sensitivity of flow stress. An increased strain-rate sensitivity has also been reported in other works investigating high strength and ductility in nanometals [1,8,17]. High strain-rate sensitivity indicates viscous flow and plays a key role in superplasticity in materials [18], but on the other hand it is associated with the development of grain-boundary sliding, and therefore depends on grain-boundary structure. This fact is in agreement with the recent results of computer simulation and studies of deformation mechanisms active in nanostructured metals. Such molecular dynamics simulations have provided valuable insight into the deformation behaviour of nanometals [19–21].

For coarse-grained metals, dislocation movement and twinning are well-known primary deformation mechanisms. But the results of simulation show that ultrafine grains may also aid in specific deformation mechanisms such as grain-boundary sliding or nucleation of partial dislocations [20–23]. Moreover, the sliding may have a co-operative (grouped) character similar to that observed in earlier studies on superplastic materials [24,25]. It should be stressed that recent experiments investigating deformation mechanisms in nanostructured materials have confirmed a number of the results of computer simulation [16,26,27].

However, there is a question: why should grain-boundary sliding in nanostructured materials, in particular in those produced by SPD, take place at relatively low temperatures? GBS is a diffusion-controlled process and usually occurs at high temperatures. A possible explanation is that diffusion may be faster in SPD-produced ultrafine-grained materials with highly non-equilibrium grain boundaries. Experiments have shown that, in SPD-produced metals, the diffusion coefficient grows considerably (by two or three orders), and this is associated with non-equilibrium grain boundaries [28,29]. So perhaps grain-boundary sliding is easier in these ultrafine-grained metals and develops during straining even at

lower temperatures, producing increased ductility. It is well known that enhanced sliding in nanostructured metals can lead even to superplasticity at relatively low temperatures [30].

Processing of nanomaterials to improve both strength and ductility is of primary importance for fatigue strength and fracture toughness [13,31,32]. An extraordinary increase in both low-cycle and high-cycle fatigue-strength may take place; there exists a theoretical explanation and the first experimental evidence of this interesting phenomenon [31,32].

3. Developing SPD techniques for effective grain refinement

HPT and equal-channel angular pressing (ECAP) are the SPD techniques that were first used to produce nanostructured metals and alloys possessing submicron- or even nano-sized grains [33,34]. Since the time of the earliest experiments, processing regimes and routes have been established for many metallic materials, including some low-ductility and hard-to-deform materials. HPT and ECAP die sets have also been essentially modernized [2,4]. Moreover, in recent years new SPD techniques have been developed, first of all twist extrusion [42], accumulative roll-bonding [43] and some others [2].

However to date, these techniques have been usually used for laboratory-scale research. The requirement of economically feasible production of ultrafine-grained metals and alloys that is necessary for successful commercialization raises several new problems in the SPD techniques development. The most topical tasks are to reduce the material waste, to obtain uniform microstructure and properties in bulk billets and products, and to increase the efficiency of SPD processing.

We solve these tasks by developing continuous ECA-pressing [35] and multi-step combined SPD processing [36] for fabrication of long-sized rods aimed at setting up commercial production of nanostructured Ti materials for medical applications. Some new results of these works are presented below.

3.1. Continuous ECA-pressing

So far, among all SPD techniques, ECAP, also known as equal-channel angular extrusion (ECAE) [37], has attracted most attention, because it is very effective in producing UFG structures and can be used to produce UFG billets sufficiently large for various structural applications [1,2,4].

However, the ECAP technique in its original design has some limitations, in particular, a relatively short length of the workpiece that makes ECAP a discontinuous process with low production efficiency and high cost. In addition, the ends of a workpiece usually contain non-uniform microstructure or macro-cracks and have to be thrown away, thus a significant portion of the workpiece is wasted and the cost of the UFG materials produced by ECAP is further increased. The key to wide commercialization of UFG materials is to lower their processing cost and waste through continuous processing. Several attempts have been made to this end. For example, repetitive corrugation and straightening (RCS) [38,39] has been

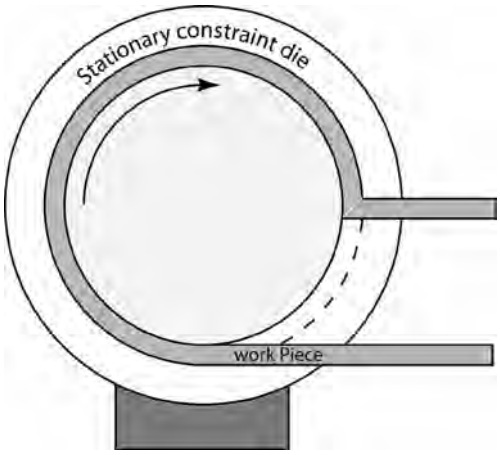

Fig. 2. Schematic illustration of an ECAP-Conform set-up

recently developed to process metal sheets and rods in a continuous manner. The co-shearing process [40] and the continuous constrained strip shearing (C2S2) process [41] were recently also reported for continuously processing thin strips and sheets to produce UFG structures. However, the question of further improvement of microstructure uniformity and properties remains topical in the development of these techniques.

In our recent studies, we have worked on combining the Conform process with ECAP to continuously process UFG materials for large-scale commercial production [35]. In this invention, the principle used to generate frictional force to push a workpiece through an ECAP die is similar to the Conform process, while a modified ECAP die design is used so that the workpiece can be repetitively processed to produce UFG structures.

We have designed and constructed an ECAP-Conform set-up which is schematically illustrated in Fig. 2. As shown in this figure, a rotating shaft in the center contains a groove, into which the workpiece is fed. The workpiece is driven forward by frictional forces on the three contact interfaces with the groove, which makes the workpiece rotate with the shaft. The workpiece is constrained to the groove by a stationary constraint die. The stationary constraint die also stops the workpiece and forces it to turn an angle by shear as in a regular ECAP process. In the current set-up, the angle is about 90°, which is the most commonly used channel intersection angle in ECAP. This set-up effectively makes ECAP continuous. Other ECAP parameters (die angle, strain rate, etc.) can also be used.

In our work [35] we used commercially pure (99.95%) coarse-grained long Al wire with a diameter of 3.4 mm and more than 1 m in length for processing at room temperature with 1–4 passes using ECAP route C, i.e. the sample was rotated 180° between ECAP passes. The starting Al wire had a grain size of 5–7 μm. Presently we are working on processing similar rods from CP Ti (Grade 2).

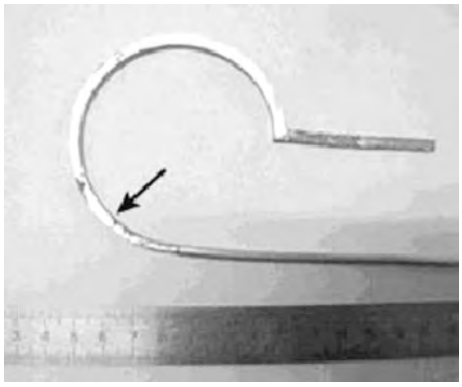

Fig. 3. Al workpiece in the process of ECAP-Conform

Fig. 3 shows an Al workpiece at each stage of the ECAP-Conform process, from the initial round feeding stock to rectangular Al rod after the first ECAP pass. As shown, the rectangular cross-section was formed shortly after the wire entered the

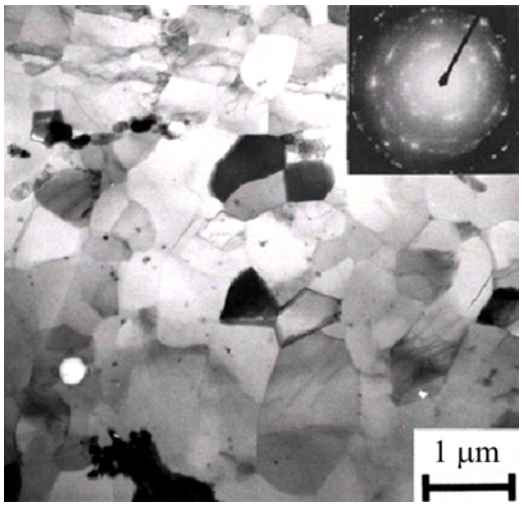

Fig. 4. TEM micrograph from the longitudinal section of Al wire processed by ECAP-Conform with four passes

groove (see the arrow mark). The change was driven by the frictional force between the groove wall and the Al workpiece. The frictional force pushed the wire forward, deformed the wire to make it conform to the groove shape. After the wire cross-section changed to the square shape, the frictional force per unit of wire length became larger because of larger contact area between the groove and the wire. The total frictional force pushed the wire forward from the groove into the stationary die channel, which intersects the groove at a 90° angle. This part of the straining process is similar to that in the conventional ECAP process.

TEM observations showed that the ECAP-Conform led to microstructure evolution typical of the ECAP process [43,44]. Fig. 4 clearly indicates that the ECAP-Conform process can effectively refine grains and produce UFG structures in Al and now in CP Ti. The tensile mechanical properties of the as-processed Al samples after 1 to 4 passes are listed in Table 1. It is obvious that the ECAP-Conform process has significantly increased the yield strength ($\sigma_{0.2}$) and the ultimate tensile strength (σ_u), while preserving a high elongation to failure (ductility) of 12–14%. These results are consistent with those for Al processed by conventional ECAP. We also found that for CP Ti there is strength growth by more than 2 times after the processing as compared with the initial material, and this fact is also consistent with Ti subjected to conventional ECAP.

Thus, the newly developed continuous SPD technique, ECAP-Conform can successfully produce UFG materials. The continuous nature of the process makes it promising for production of UFG materials on a large scale, in efficient and cost effective manner. However, further study is needed to investigate its ability with respect to grain refinement and properties improvement of various UFG materials.

Table 1

Yield strength $\sigma_{0.2}$, ultimate tensile strength σ_u, elongation to failure δ, and cross-section reduction (necking) ψ of Al samples processed with 1 to 4 passes

Processing state	$\sigma_{0.2}$, MPa	σ_u, MPa	δ, %	ψ, %
Initial Al rod	47	71	28	86
After 1 pass	130	160	13	73
After 2 passes	140	170	12	72
After 3 passes	130	160	14	76
After 4 passes	140	180	14	76

3.2. Combined SPD processing

While solving the problem of fabrication of nanostructured Ti materials for medical applications we showed the advantage of combining ECAP with other techniques of metal forming such as rolling, forging or extrusion [45,46]. These advantages are connected with effective shaping of long-sized semiproducts (sheets, rods) as well as further enhancement of properties of UFG materials. For example, in Grade 2 CP Ti high strength (YS = 980 MPa, UTS = 1100 MPa) with elongation to failure δ = 12% was attained using ECAP and extrusion. Also the results of investigations on processing of Ti rods of over 800 mm in length and 6.5 mm in diameter by a combination of ECAP and thermomechanical treatment (TMT) including forging and rolling are very impressive [36].

Fig. 5 presents TEM micrographs of CP Ti subjected to ECAP + TMT, 80%. It can be seen that the combined processing results in significant additional grain refinement down to 100 nm in comparison with 30–400 nm after ECAP; however, a considerable elongation of grains takes place. Mechanical testing has shown (Table 2) that TMT after ECAP results in strength growth of CP Ti and the record values of $\sigma_{0.2}$ and σ_u are observed; at the same time, sufficient ductility is preserved. It is important that these strength values of nanostructured CP Ti are visibly higher than those of the Ti–6%Al–4%V alloy that is presently widely used in medicine and engineering.

It is also interesting that the microstructure and properties of the obtained rods are rather uniform, the dispersion of mechanical properties along the rod length does not exceed ±5% [11]; at the same time material waste totals 0.65. This shows great prospects for the use of combined SPD processing for commercial production of semi-products from Ti for medical application.

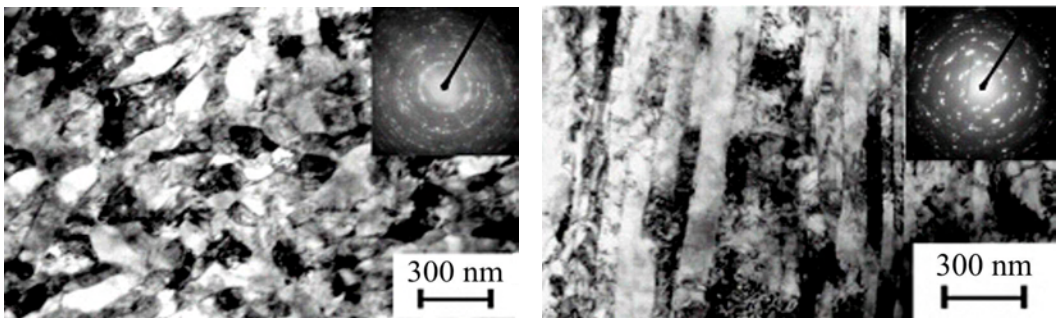

a *b*

Fig. 5. TEM micrographs displaying the microstructure of Grade 2 Ti after ECAP + TMT, 80%: *a* – cross-section; *b* – longitudinal section

Table 2

Mechanical properties of Grade 2 Ti billets at different stages of processing

State	σ_u, MPa	$\sigma_{0.2}$, MPa	δ, %	ψ, %
Initial	440	370	38	60
ECAP, 4 passes	630	545	22	51
ECAP, 4 passes + TMT, ε = 80%	1150	1100	11	56

4. Using SPD-produced nanostructured metals

Markets for bulk nanostructured materials exist in virtually every product sector where superior mechanical properties (in particular, strength, strength-to-weight ratio and fatigue life) are critical design parameters. Formal market analyses, conducted by companies such as Metallicum, that specialize in nanostructured materials, have identified over 100 specific markets for nanometals in aerospace, transportation, medical devices, sports products, food and chemical processing, electronics and conventional defense [47]. Among them we can single out the following directions: 1) development of extra-strong nanostructured light alloys (Al,Ti,Mg), for example Al-based commercial alloys with yield strength over 800–900 MPa, for the motor industry and aviation; 2) development of metals and alloys with ultrafine-grained structure for use at cryogenic temperatures [48]; 3) development of nanostructured ductile refractory metals and high-strength TiNi alloys with advanced shape-memory effect for space, medical and other applications. The applications of nanostructured materials in engineering new-generation aviation engines [49] or in high-strain-rate superplastic forming of complex-shaped parts for new automobiles and planes [50] are worth a special mention.

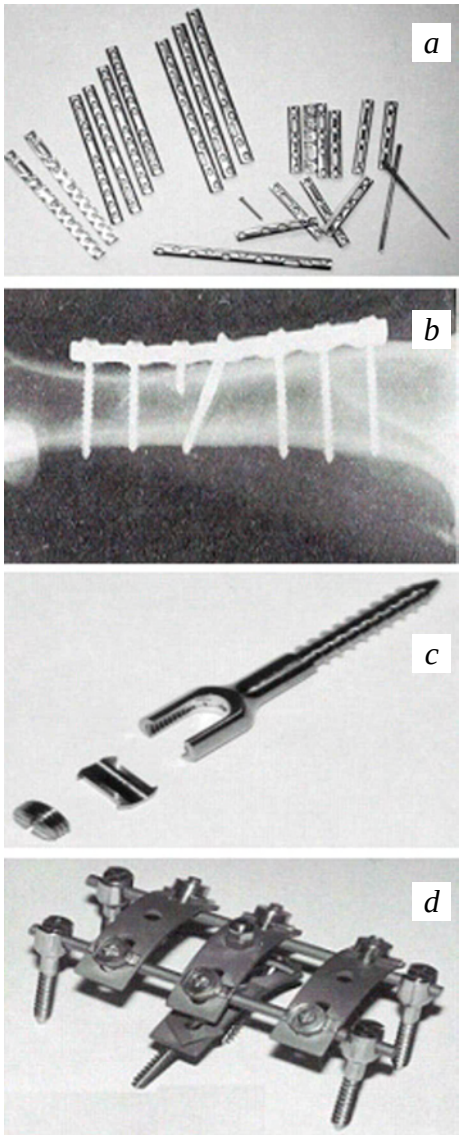

Fig. 6. Medical implants made of nanostructured titanium: *a*, *b* – plate implants for osteosynthesis; *c* – conic screw for spine fixation; *d* – device for correction and fixation of spinal column

Out of the broad range of possible applications of advanced nanostructured metals, we focus here on the one that is representative of the high-tech market: biomedical implants and devices. High mechanical and fatigue properties are the essential requirements for metallic biomedical materials, in particular titanium and its alloys [51], which have excellent biological compatibility and high biomechanical properties. For example, in trauma cases, plates and screws made of new titanium materials are planned to be widely used for fixing bones. These plates need very high compressive and bending strength, and sufficient ductility. Different implant-plate constructions for osteosynthesis have been analysed, resulting in the design and processing of a series of nanostructured titanium plates (Fig. 6,*a*,*b*). Fig. 6,*c* illustrates an-

other application of nanostructured titanium for a special conic screw, which requires high fatigue strength as well. In this case all the advantages of nanostructured titanium are fully used [46] – high static and fatigue strength (yield tensile strength ≥ 950 MPa at strain rate 10^{-3} s^{-1}, endurance of more than 500 MPa at $2 \cdot 10^7$ cycles) and excellent biological compatibility.

5. The new SPD processing of bulk nanocrystalline materials

Since the first works dating back to the early 1990s [33,34], SPD techniques have been used mostly because of their ability to produce ultrafine-grained materials through microstructure refinement in initially coarse-grained metals [2]. The final grain size produced depends strongly on both processing regimes and the type of material. For pure metals the mean grain size is typically about 100–200 nm after processing by HPT and about 200–300 nm after processing by ECAP. For alloys and intermetallics the grain size is usually less and in some cases it equals 50–100 nm. However, it is very important for fundamental tasks and many advanced applications to have bulk nanocrystalline materials with a mean grain size less than 30–50 nm. Is it possible to produce such materials using SPD techniques? In recent years this problem has become the object of special investigations in our laboratory where we are developing two approaches: SPD consolidation of powders and SPD-induced nanocrystallization of amorphous alloys.

5.1. SPD consolidation

Already in the early work on consolidation of powders [52,53] it was revealed that during HPT high pressures of several GPa can provide a rather high density close to 100% in the processed disc-type nanostructured samples. For fabrication of such samples via severe torsion straining consolidation not only conventional powders but also powders prepared by ball milling can be used.

HPT consolidation of nanostructured Ni and Fe powders prepared by ball milling [52,53] can be taken as an example. The conducted investigations showed that the density of the samples processed at room temperature is very high and close to 95% of the theoretical density of bulk coarse-grained metals. After HPT consolidation at 200 or 400°C the samples density is even higher and reaches 98%. TEM examinations showed the absence of porosity. The mean grain size is very small; it is equal to 17 nm and 20 nm for Ni and Fe, respectively. It is also very interesting that the value of microhardness of the Ni samples produced by HPT consolidation was 8.60 ± 0.17 GPa, the highest value of microhardness mentioned in literature for nanocrystalline Ni.

5.2. SPD-induced nanocrystallization

Recent investigations also show that SPD processing can control crystallization of initially amorphous alloys that may result in the formation of bulk nanocrystalline alloys with a very small grain size and new properties [54,55]. In the present paper this approach is used to produce and to investigate nanocrystalline

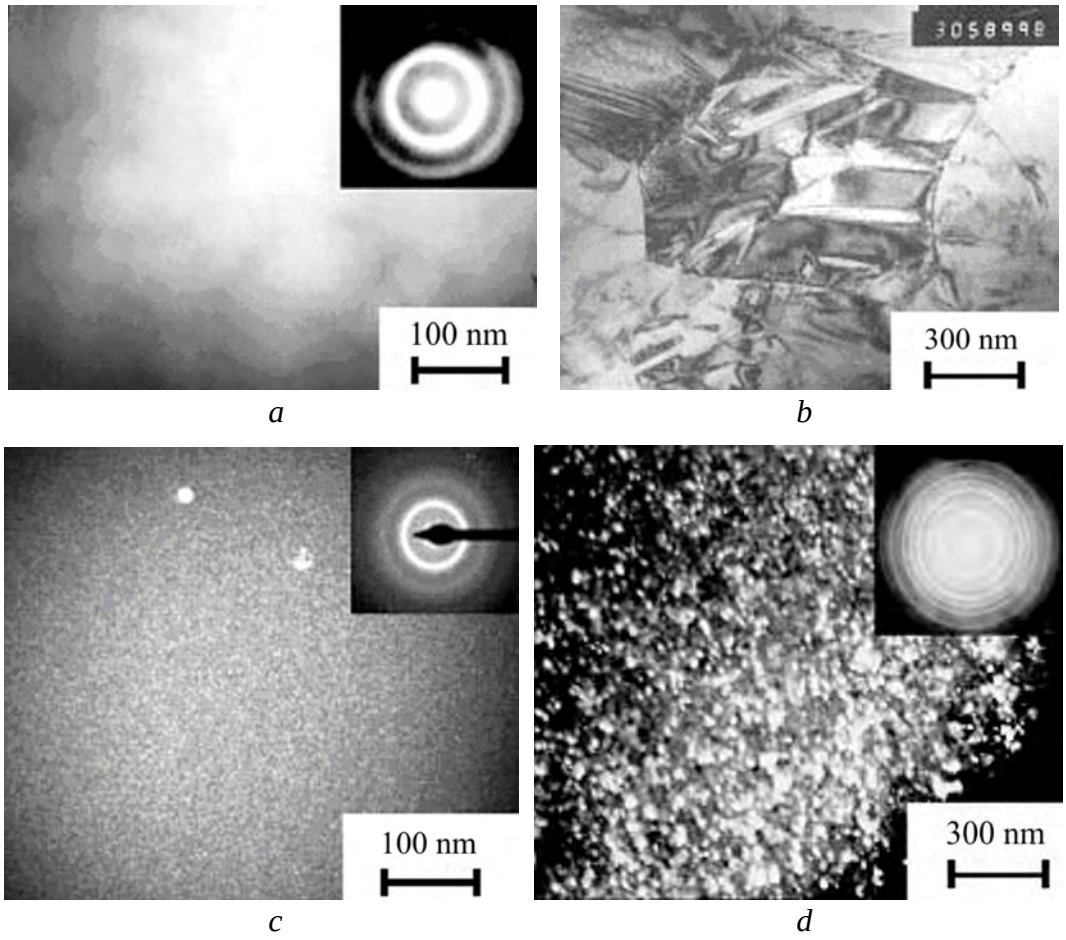

a *b* *c* *d*

Fig. 7. TEM image of rapidly-quenched alloy $Ti_{50}Ni_{25}Cu_{25}$: *a* – initial state (dark field); *b* – after annealing at 450°C for 10 min; *c* – after HPT (dark field); *d* – after HPT and annealing at 390°C for 10 min

Ti–Ni alloys widely known as alloys with shape memory effects. As the material for this investigation, two alloys of the Ti–Ni system were used: melt-spun $Ti_{50}Ni_{25}Cu_{25}$ alloy [55,56] and cast $Ti_{49.4}Ni_{50.6}$ alloy [57,58].

The amorphous structure of $Ti_{50}Ni_{25}Cu_{25}$ alloy was confirmed by TEM and X-ray investigations (Figs 7, 8) [55,56]. However, after HPT at room temperature, although the diffraction methods still indicated the amorphous structure of the alloy, TEM studies showed the appearance of many nanocrystals with very small sizes of about 2–3 nm (Fig. 7,*c*).

The essential difference in behaviour of this alloy in the amorphous state and after HPT was revealed during subsequent annealing. As it can be seen in Fig. 8, the amorphous alloy was crystallized at 450°C, then, while cooling, a martensite phase B19 was forming. According to TEM, the microstructure of the alloy after annealing is rather non-uniform and together with small grains it contains large grains with a size of almost about 1 micron (Fig. 8,*c*). At the same time after HPT crystallization occurs below 390°C and it appears possible to produce a uniform nanocrystalline structure with a grain size of under 50 nm (Fig. 7,*d*). It is rather

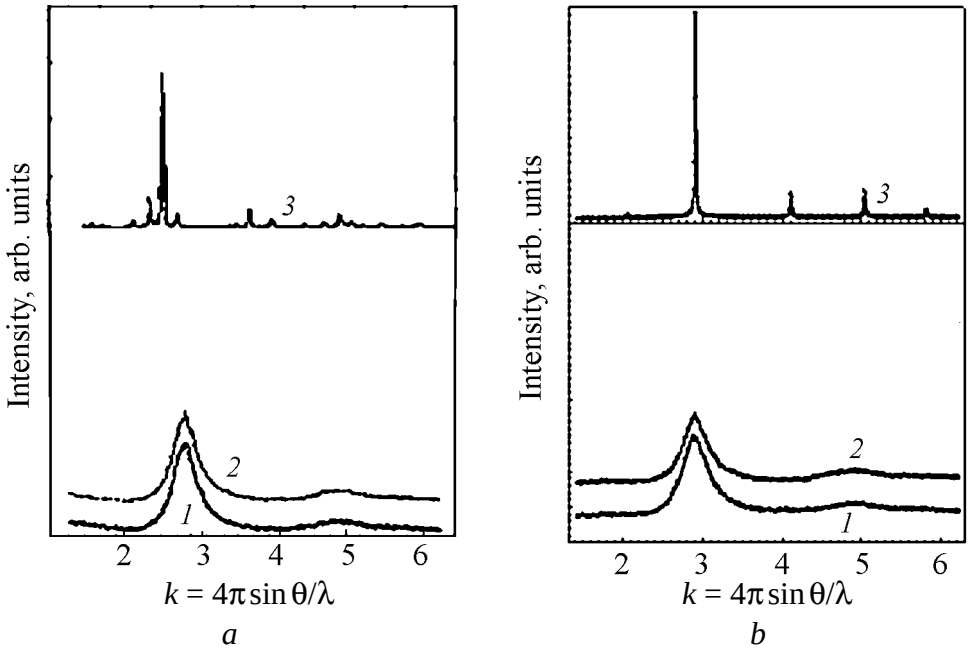

Fig. 8. X-ray diffraction patterns of the $Ti_{50}(Ni,Cu)_{50}$ alloy: *a* – initial rapidly-quenched alloy (*1*), after annealing at 300°C for 5 min (*2*), after annealing at 450°C for 5 min (*3*) with the phase B19; *b* – alloy after HPT (*1*), after HPT and annealing at 300°C for 5 min (*2*), after HPT and annealing at 400°C for 5 min, with the phase B2 (*3*)

interesting that the structure after cooling is an austenitic B2-phase; in other words, imposing severe plastic deformation on the amorphous alloy has effected the alloy crystallization during the heating process and changed its phase composition after the annealing and further cooling to the room temperature.

In the coarse-grained alloy $Ti_{50}Ni_{25}Cu_{25}$, the temperature of martensite transformation upon cooling equals ~ 80°C, that is why there is a martensite phase in the alloy at room temperature. In this connection, the existence of only austenitic phase after HPT and nanocrystallization can be related to the martensite transformation retard in the alloy with a nanocrystalline grain size. This fact was previously reported in the literature for ultrafine-grained Ti–Ni alloys [59]. Speaking about the alloy $Ti_{50}Ni_{25}Cu_{25}$, the critical point is the grain size of about 100 nm. Martensite transformation does not take place at room temperature below this size.

The amorphous state in the $Ti_{49.4}Ni_{50.6}$ alloy can be obtained directly as a result of HPT processing (P = 6 GPa, n = 5 revolutions) [57,58]. Then the homogeneous nanocrystalline structure was produced by annealing of the HPT material (Fig. 9). For instance, after annealing at 400°C for 0.5 h the mean grain size is about 20 nm (Fig. 9,*a*,*b*), and after annealing at 500°C it is about 40 nm (Fig. 9,*c*,*d*). It is worth to mention that according to HREM observations after such annealing there are no regions of amorphous phase and grain boundaries are well defined, although there are still small distortions of the crystal lattice near some of the boundaries.

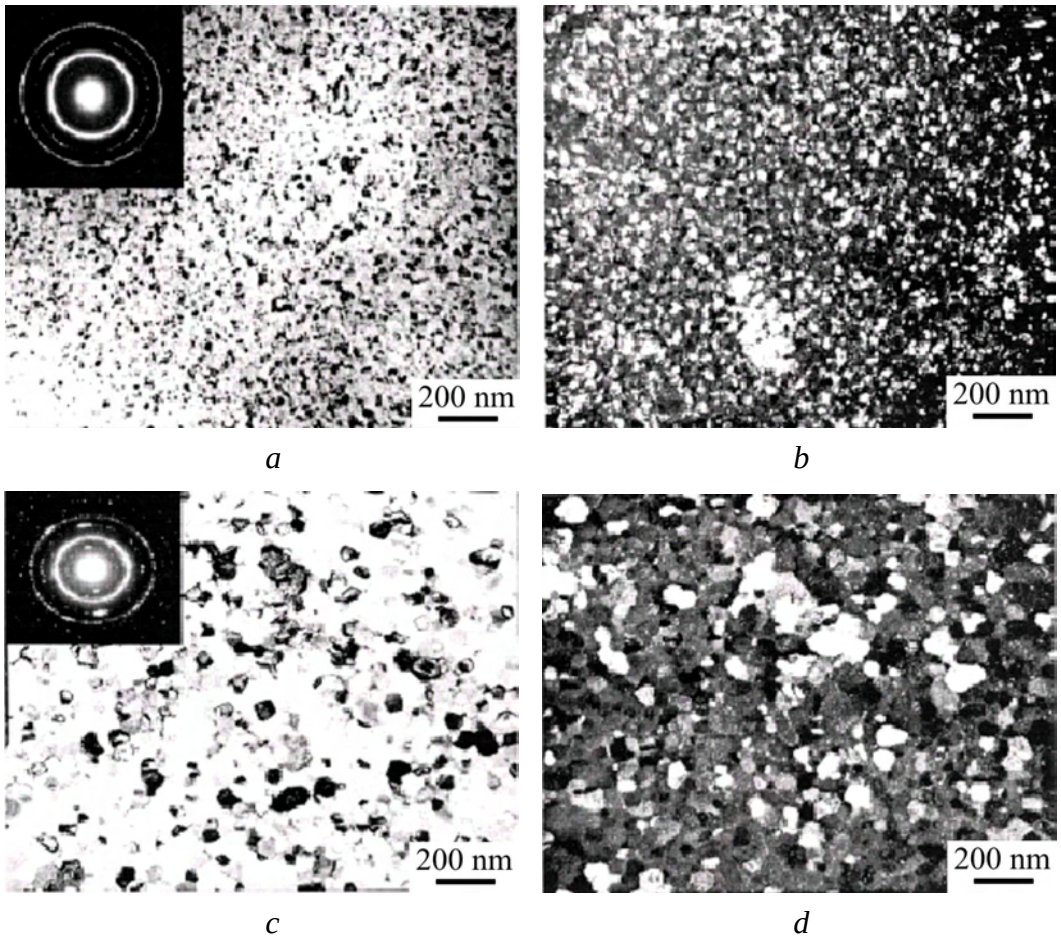

Fig. 9. TEM micrographs of $Ti_{49.4}Ni_{50.6}$ alloy after HPT and annealing at 400°C (*a*, *b*) and at 500°C (*c*, *d*) for 0.5 h: *a*, *c* – bright field images; *b*, *d* – dark field images

Tensile mechanical tests showed that the amorphous nitinol produced by HPT had much higher strength in comparison with the initial microcrystalline state [57], but it was essentially brittle. Nanocrystallization results in the record value of strength for this material equal to 2650 MPa with an elongation to failure of about 5%.

Thus, SPD consolidation of powders and SPD-induced nanocrystallization can be considered as new SPD processing routes for fabrication of bulk nanocrystalline materials. One of the advantages of this technique is the possibility of producing fully dense samples with a uniform ultrafine-grained structure having a grain size less than 40–50 nm. Studies of the properties of these materials are of great interest for ongoing research because deformation mechanisms and, as mentioned above, phase transformations can basically change in materials with a small grain size [7,60].

6. Conclusions

Several new trends in SPD processing for fabrication of bulk nanostructured materials have been presented in this article, based on recent results of our works on the development of commercial technology of nanostructured Ti materials production for medical and some other applications. We demonstrate how new tasks,

connected with economically feasible production of UFG metals and alloys, can be solved by decreasing the material waste, obtaining homogeneous structure and advanced properties in bulk billets and products.

From the fundamental point of view, investigations focused on fabrication of bulk nanocrystalline materials using SPD techniques are of continuous interest. This paper also presented the two new approaches – SPD consolidation of powders and SPD-induced crystallization – both rising hopes for a successful resolution of this important manufacturing problem.

The present paper was supported in part by the NIS-IPP Program of DOE (USA) and the Russian Foundation for Basic Research. Cooperation with co-authors mentioned in references is gratefully acknowledged as well.

1. *R.Z. Valiev, R.K. Islamgaliev, I.V. Alexandrov*, Prog. Mater. Sci. **45**, 103 (2000).
2. *R.Z. Valiev, Y. Estrin, Z. Horita, T.G. Langdon, M.J. Zehetbauer, Y.T. Zhu*, JOM **58**, № 4, 33 (2006).
3. *Ultrafine* Grained Materials II, Y.T. Zhu, T.G. Langdon, R.S. Mishra, S.L. Semiatin, M.J. Saran, T.C. Lowe (Eds), TMS (The Minerals, Metals and Materials Society), Warrendale, PA, USA (2002).
4. *T.C. Lowe, R.Z. Valiev*, JOM **56**, № 10, 64 (2004).
5. *Ultrafine* Grained Materials III, The Minerals, Metals and Materials Society, *Y.T. Zhu et al.* (Eds.), Warrendale, PA, USA (2004).
6. *Special* Issue on Nanomaterials by Severe Plastic Deformation (SPD), M. Zehetbauer (Ed.), Adv. Eng. Mater. **5** (2003).
7. *R.Z. Valiev*, Nature Mater. **3**, 511 (2004).
8. *R.Z. Valiev, I.V. Alexandrov, Y.T. Zhu, T.C. Lowe*, J. Mater. Res. **17**, 5 (2002).
9. *R. Valiev*, Nature **419**, 887 (2002).
10. *Y. Wang, M. Chen, F. Zhou, E. Ma*, Nature **419**, 912 (2002).
11. *Y.M. Wang, E. Ma*, Acta Mater. **52**, 1699 (2004).
12. *X. Zhang et al.*, Acta Mater. **50**, 4823 (2002).
13. *H. Mughrabi, H.W. Höppel, M. Kautz, R.Z. Valiev*, Z. Metallkunde **94**, 1079 (2003).
14. *Y.S. Park, K.H. Chung, N.J. Kim, E.J. Lavernia*, Mater. Sci. Eng. **A374**, 211 (2004).
15. *C.C. Koch*, Scripta Mater. **49**, 657 (2003).
16. *R.Z. Valiev, A.V. Sergueeva, A.K. Mukherjee*, Scripta Mater. **49**, 669 (2003).
17. *R.Z. Valiev et al.*, Acta Metall. Mater. **42**, 2467 (1994).
18. *T.G. Nieh, J. Wadsworth, O.D. Sherby*, Superplasticity in Metals and Ceramics, Cambridge Univ. Press, Cambridge (1997).
19. *H. Van Swygenhoven*, Science **296**, 66 (2002).
20. *V. Yamakov, D. Wolf, S.R. Phillpot, A.K. Mukherjee, H. Gleiter*, Nature Mater. **1**, 1 (2002).
21. *J. Schiötz, K.W. Jacobsen*, Science **301**, 1357 (2003).
22. *Z. Budrovic, H. Van Swygenhoven, P.M. Derlet, P. Van Petegem, B. Schmitt*, Science **304**, 273 (2004).
23. *H. Van Swygenhoven, P.M. Derlet, A.G. Fröseth*, Nature Mater. **3**, 399 (2004).

24. *M.G. Zelin et al.*, Acta Metall. Mater. **42**, 119 (1994).
25. *H. Hahn, K.A. Padmanaban*, Phil. Mag. **B76**, 559 (1997).
26. *M. Chen et al*., Science **300**, 1275 (2003).
27. *X.Z. Liao et al*., Appl. Phys. Lett. **83**, 5062 (2003).
28. *Yu.R. Kolobov et al*., Scripta Mater. **44**, 873 (2001).
29. *R. Würschum, S. Herth, U. Brossmann*, Adv. Eng. Mater. **5**, 365 (2003).
30. *S.X. McFadden, R.S. Mishra, R.Z. Valiev, A.P. Zhilyaev, A.K. Mukherjee*, Nature **398**, 684 (1999).
31. *H.W. Höppel, Z.M. Zhou, H. Mughrabi, R.Z. Valiev*, Phil. Mag. **A82**, 1781 (2002).
32. *A. Vinogradov, S. Hashimoto*, Adv. Eng. Mater. **5**, 351 (2003).
33. *R.Z. Valiev, N.A. Krasilnikov, N.K. Tsenev*, Mater Sci. Eng. **A137**, 35 (1991).
34. *R.Z. Valiev, A.V. Korznikov, R.R. Mulyukov*, Mater Sci. Eng. **A186**, 141 (1993).
35. *G.J. Raab, R.Z. Valiev, T.C. Lowe, Y.T. Zhu*, Mat. Sci. Eng. **A382**, 30 (2004).
36. *V.V. Latysh, I.P. Semenova et al*., Proc. of $NanoSPD_3$ conference, Uetikon-Zuerich, eds. Z. Horita (2005), p. 763.
37. *V.M. Segal*, Mater. Sci. Eng. **A197**, 157 (1995).
38. *J. Huang, Y.T. Zhu, H. Jiang, T.C. Lowe*, Acta Mater. **49**, 1497 (2001).
39. *Y.T. Zhu, H. Jiang, J. Huang, T.C. Lowe*, Metall. Mater. Trans. **A32**, 1559 (2001).
40. *Y. Saito, H. Utsunomiya, H. Suzuki, T. Sakai*, Scripta Mater. **42**, 1139 (2000).
41. *J.C. Lee, H.K. Seok, J.Y. Suh*, Acta Mater. **50**, 4005 (2002).
42. *Y. Beygelzimer, D. Orlov, V. Varyukhin*, Ultrafine Grained Materilas II, Y.T. Zhu, T.G. Langdon, R.S. Mishra, S.L. Semiatin, M.J. Saran, T.C. Lowe (Eds), TMS (The Minerals, Metals & Materials Society) (2002), p. 297.
43. *Y. Saito, H. Utsunomiya, N. Tsuji, T. Sakai*, Acta Mater. **47**, 579 (1999).
44. *M. Furukawa, Z. Horita, M. Nemoto, T.G. Langdon*, J. Mater. Sci. **36**, 2835 (2001).
45. *V.V. Stolyarov, Y.T. Zhu, T.C. Lowe, R.Z. Valiev*, Mater. Sci. Eng. **A303**, 82 (2001).
46. *Yu.T. Zhu, T.C. Lowe, R.Z. Valiev, V.V. Stolyarov, V.V. Latysh, G.I. Raab*, U.S. Patent 6, 399, 215 (2002).
47. *T.C. Lowe, Y.T. Zhu*, Adv. Eng. Mater. **5**, 373 (2003).
48. *Y. Wang, E. Ma, R.Z. Valiev, Y.T. Zhu*, Adv. Mater. **16**, 328 (2004).
49. *M. Gell*, JOM **46**, 30 (1994).
50. *C. Xu, M. Furukawa, Z. Horita, T.G. Langdon*, Acta Mater. **51**, 6139 (2003).
51. *D.M. Brunette, P. Tengvall, M. Texto, P. Thomen*, Titanium in Medicine, Springer, Berlin and Heidelberg (2001).
52. *R.Z. Valiev, R.S. Mishra, J. Grosa, A.K. Mukherjee*, Scripta Mater. **34**, 1443 (1996).
53. *R.Z. Valiev*, Proc. of $NanoSPD_3$ conference, Uetikon-Zuerich, eds. Z. Horita, 3 (2005).
54. *R.Z. Valiev*, Adv. Eng. Mat. **5**, 296 (2003).
55. *G. Wilde, N. Boucharat, G.P. Dinda, H. Rösner, R.Z. Valiev*, in: Proc. of $NanoSPD_3$ conference, Uetikon-Zuerich, eds. Z. Horita (2005), p. 425.
56. *R.Z. Valiev, D.V. Gunderov et al*., Doklady RAN **398**, 1 (2004).
57. *A.V. Sergueeva, C. Song, R.Z. Valiev, A.K. Mukherjee*, Mat. Sci. Eng. **A339**, 159 (2003).
58. *J.Y. Huang, Y.T. Zhu, X.Z. Liao, R.Z. Valiev*, Phil. Mag. Lett. **84**, 183 (2004).
59. *T. Waitz, V. Kazykhanov, H.P. Karnthaler*, Acta Mater. **52**, 385 (2004).
60. *Y.T. Zhu, T.G. Langdon*, JOM **56**, № 10, 58 (2004).